REVIEW OF RESEARCH
ISSN: 2249-894X
IMPACT FACTOR : 5.7631(UIF)
VOLUME - 14 | ISSUE - 8 | MAY - 2025

A SYSTEMATIC STUDY OF SYNTHESIS, CHARACTERIZATION AND GAS SENSING OF ZINC OXIDE AND COPPER OXIDE THICK FILMS BY VARIOUS DEPOSITION TECHNIQUES

Mr. Sudhakar V. Maske
I.C.S. College of Arts, Commerce and Science, Khed,
Dist. Ratnagiri.(Maharashtra)

ABSTRACT :

This paper presents a systematic study on the synthesis, characterization, and gas sensing performance of zinc oxide (ZnO) and copper oxide (CuO) thick films made using different deposition techniques. The films were prepared using methods such as screen printing, doctor blade, and sol-gel coating. Structural and surface properties were analyzed using X-ray diffraction (XRD), scanning electron microscopy (SEM), and energy-dispersive X-ray spectroscopy (EDX). The gas sensing behavior of the films was tested against gases like ammonia (NH_3), ethanol (C_2H_5OH), and nitrogen dioxide (NO_2) at various temperatures. Results show that the deposition technique greatly affects the film's microstructure and sensing ability. Among the methods, [insert best-performing method here] showed the highest sensitivity, better selectivity, and faster response and recovery times. This study highlights the potential of ZnO and CuO thick films for use in reliable and efficient gas sensors in environmental and industrial monitoring.

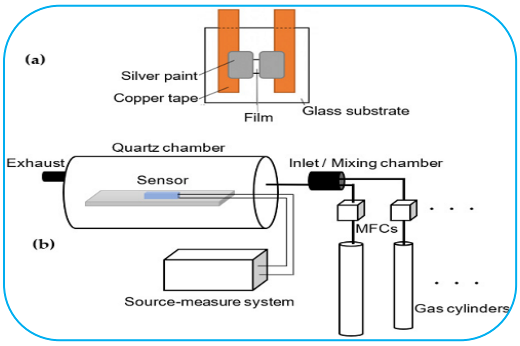

KEYWORDS : *Zinc oxide (ZnO), Copper oxide (CuO), Screen printing, Sol-gel, Structural characterization, SEM, XRD.*

1 INTRODUCTION

Thick-film technology is simultaneously one of the oldest arts and one of the newest sciences. Thick film microelectronics and optoelectronics are among the strongest technological driversof our economy, a fact manifested by the explosive growth in communications and information processing, storage and display applications. Technologies have fertilized expanding thick filmuses in diverse areas e.g., coating of all kinds, bio-technology and the generation and conservation of energy. Thick film applications are issues rooted in material science and engineering. Involvement with thick films dates to the metal ages of antiquity. The processing of materials into thick films allows easy integration into various types of devices. Theproperties of material significantly differ when they are analyzed in the form of thick films. Most of the functional materials are rather applied in thick film form due to their specific electrical, magnetic, optical properties or wear resistance.

2 THICK FILMS

It can be observed that droplets of the liquid/ semi solid/ solid on the surface of the water formsa layer that ranges in a few micrometers. Also, the soap water forms bubbles on the top of that are nanometer (nm) to micrometer (~µm) in thickness. Multicolor reflections of light from the surface of CDs are because of the thin layer of magnetic materials deposited over the sturdy plastic substrate body. It is crucial to talk about the concept of being "thin" in relation to the development of layers in surface engineering. It can be challenging to define a thick film because some people may consider 300 nanometers to be thick, while others may consider 1 to2 nanometers to be equally thin. The concept of thinness depends on the applications for a given material; from there, we may determine if the material is thin or thick. Therefore, the size may be in the nanometer range or occasionally in the micrometer range depending on how thinit is. However, there are times when the literature will indicate the monetary value of 1 m. When a film's structural, electrical, optical, magnetic, and other physical characteristicsconsiderably diverge from the underlying bulk layer, the film is said to be thick. For instance, films made of indium oxide (In2O3), which have high transmissions in the visible spectrum and high reflectivity in the infrared, could be utilized as a material for thermal coating. This may be because optical interference effects need a material thickness of about 300 nm, which leads us to think of 300 nm as a thin material for optical applications.

Figure 1. Miniaturization of materials towards thick film

The picture shows how the material is dynamic dependent on its shape, structure, and physical dimensions, which encourages a variety of uses and improves its usefulness.

3. PROPERTIES OF THICK FILM

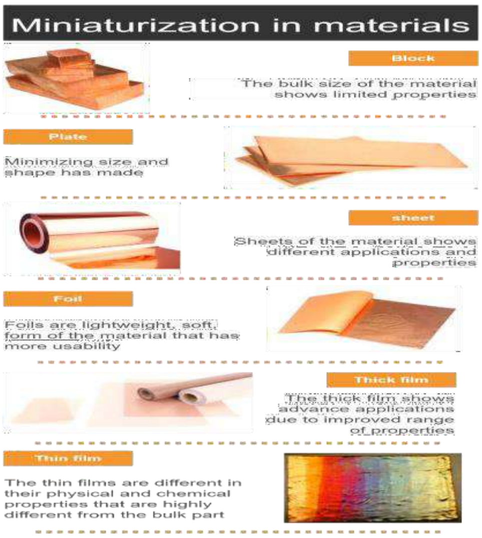

The properties of the thin films are different from the bulk material.

- Film that is thick need not be dense.
- Thick films continue to be stressed.
- Different structural geometry is processed by thick films than by bulk materials.
- Thick films are almost three-dimensional in design.
- The surface/interface effects have a significant impact on thick films.

Due to these fundamental property modifications, the thin films were only capable of experiencing significant modifications to their measurably quantifiable structural, electric, electromagnetic, dielectric, magnetic, optical, and mechanical properties.

3.1 Developing the thick film

According to technological development, there are three main stages to the thick film deposition process. Production of the suitable atomic, molecular, or ionic species is referred toas the first step. The second step involves moving these components via a medium and onto the substrate. The third method is condensation, which can generate solid deposits directly on the substrate or indirectly through a chemical or electrochemical reaction.

3.2 Growth stages in the thick film

The growth stages involved the nucleation processes and the development stages in the various thick film deposition techniques. These phases are dependent on the numerous deposition circumstances, including substrate chemistry, growth temperature, and growth rate.

3.3 Need of thick film deposition

In order to satisfy a specific requirement or accomplish a specific objective, such as maintaining surface uniformity, lowering the amount of light-absorbing material, decreasing the bulkiness of the material, or lowering the material's weight, a thick film must be developed.

4 THICK FILM DEPOSITION TECHNIQUE

Researchers have created a variety of deposition processes throughout the years to meet the demands of various sectors, R&D fields, human living ecosystems, and platforms for the future. These deposition techniques have been divided into *Physical* and *Chemical* categories for easier comprehension.

The physical deposition process is typically used to create single component films, such as metal films. The graphic illustrates how several specialized procedures used in the evaporation and sputtering mechanisms are also included in the physical deposition method. One can choose soft solutionchemical processes for the creation of advanced inorganic materials such as perovskite-type oxide, spinel oxide, nanowires and Nano dot with a quantum size effect, etc. to fulfil specific goals in the deposition and get around the constraints of physical methods. The idea behind the chemical deposition process is based on the idea that the chemical solution controls how quickly the film grows. The design and functionality of the film are significantly influenced bythe chemical processes taking place on the substrate's surface or in its immediate vicinity. The gas phase and liquid phase have the potential to influence the chemical deposition process. Electro-deposition, chemical bath deposition (CBD), sequential ionic layer adsorption and reaction (SILAR), electroless deposition, anodization, spray pyrolysis technique (SPT), liquidphase epitaxy, and sol-gel are a few examples of liquid phase deposition [17]. Different Chemical deposition techniques in the gas phase include chemical vapour deposition (CVD), laser-induced chemical vapour deposition (LCVD), photo-chemical vapour deposition (P- CVD), metal organo-chemical vapour deposition (MO-CVD), and plasma-enhanced chemicalvapour deposition (PE-CVD) [18].

Figure 2. Different approaches for the deposition of thick film techniques

According to the physical and chemical approaches to deposition, thick film depositiontechniques have generally been categorized as illustrated in the **figure 2**.

5 SENSING DEVICES

A wide range of sensors, including semiconductor gas sensors [19], optical sensors [20], thermal conductivity sensors [21], mass-sensitive devices [22] like quartz microbalance sensors [23], catalytic sensors [24], dielectric sensors [25], electrochemical sensors [26], and electrolyte sensors [27] have all been developed based on various sensing principles [28]. some of the functionalization of the most common sensors are mentioned:

Pressure sensors can quantify force per unit surface and detect variations in pressure in gases and liquids.Temperature sensors can determine the temperature of an object or the surrounding surroundings and track variations. Chemical monitors can identify the existence of chemicals in the surrounding area. Motion sensors can recognise when a tangible item is moving. Proximity devices can estimate an object's distance. Water quality monitors can examine the oxygen and PH levels, electrical conductivity, and existence of chemicals in the water. Smoke monitors can identify whether there is smoke on the property. Heat and infrared emission levelscan be measured by infrared (IR) instruments. The level of liquids, powders, and granular solids in containers can be measured using level monitors. Images can be captured by picture sensorsfor later processing and analysis. Motion devices can gauge an object's motion. By detecting the angular motion of an item, gyroscopic devices can identify its orientation. Utilizing the sensing of light reflection, optical devices can identify things. Sensor elements must meet certain requirements in order for sensor systems to be portable, affordable, or useful for air quality monitoring. These requirements include: low power requirements; compatibility with straightforward sampling systems; the absence of the need for external carriers or reactant gases; small size and, if possible, compatibility with microelectronic technologies; reversible and reproducible responses; adequate sensitivity [29].

5.1 ZnO Thick film

ZnO thick films have been grown using variety of deposition techniques, including spray pyrolysis, vacuum evaporation, chemical vapor deposition, magnetron sputtering, pulsed laser deposition, the sol-gel process, and screen printing. In the latter half of the 1950s, the screen printing method was developed to create versatile, robust, and reasonably priced hybrid circuits. Later, the sensor field was drawn to the thick film method. A practical and affordable technique for creating thick films out of a variety of materials is screen printing. Additionally, ZnO's thermal expansion coefficient matches that of alumina, making it appropriate for the creation of thin- or thick-film-based instruments.

5.2 Crystal structure of Zinc oxide (ZnO)

The breaking down of solid materials into small pieces by applying external force in this approach many physical-chemical and thermal techniques are used to provide the necessary energy for nanoparticle formation however with the method it is difficult to expected narrow size. Naturally crystallized zinc oxide represents a wurtzite structure that corresponds to the space group P63mc, ZnO unit cell wurtzite structure and various crystal planes as shown in **figure 3(a), (b) and (b)** for the schematic illustration of the cubic rock salt, cubic zincblende, and hexagonal wurtzite ZnO crystal formations. To emphasize the stacking order, the links in the (110) and (1120) planes that are darkened are shown with thicker lines. The bond length or closest neighbor distance b split by c for the wurtzite structure is 0.375, and in the ideal crystal, the bond angles and are 109.47 degrees.

6. EXPERIMENTAL TECHNIQUE

6.1 Materials

All reagents-Zinc Chloride (ZnCl2), Cupric Nitrate Trihydrate Cu(No3)2.3H2O, and Sodium Hydroxide(NaOH)- with analytical grade (AG) were used in this work without any added efinement and were purchased from Molychem, India.

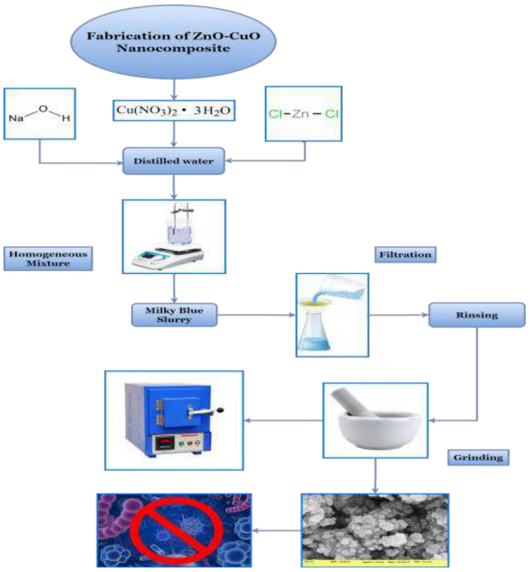

Figure 6. Synthesis of ZnO-CuO nanoparticles

6.2 Preparation of ZnO-CuO NCPs thick film

The ZnO-CuO NCPs thick film with different concentrations 8:2, 7:3, 6:4, and 5:5 has been prepared using wet-chemical method. To prepare ZnO80%-CuO20% NCP, 0.4 ml of ZnCl2 solution was prepared in 100 ml of distilled water with a magnetic stirrer for 20 min. Then 0.2M of

$Cu(NO3)2.3H2O$ was added into the previous solution with a continued stirring process for 20 min till obtained blue mixture was. On the other side, 1 ml of NaOH solution was prepared in 100 ml of distilled water with a magnetic stirrer for 20 min. NaOH solution was added drop wise into the previous mixture with a continued stirring process till obtained milky blue mixture was. This milky blue mixture obtained was filtered and rinsed several times with distilled water. It was dried for 48 h at room temperature. To obtain fine nanostructures, the product was crushed well using a pestle. Finally, it was calcined at 380°C for 3 h in the furnace to obtain a blackish-brown powder of ZnO80%-CuO20% NCP. The process of fabrication using co-precipitation method is depicted in **Figure 1** and it was repeated with the remaining ZnO-CuO NCPs thick film in percentage; ZnO70%-CuO30%; ZnO60%-CuO40%; and ZnO50%- CuO50%. Through the calcination process, the metals oxide Nanocomposite were obtained assuming the following reaction:

6.3 Characterization of ZnO-CuO NCPs thick film

X-Ray diffraction pattern (XRD) of ZnO NPs and ZnO-CuO NCPs thick film were characterized by MiniFlex from Rigaku with target metal Cuα-radiation at a wavelength (λ) of 1.54060 Å; scanning range of 2θ from -3° to 145°; maximum power 600 W; voltage 40 kV; and current 15 mA; with a scanning rate 2 degree/min. The functional groups and fingerprint groups of the samples were identified using the Fourier Transform Infrared Spectrophotometer (FTIR) Shimadzu, IRAffinity-1S with a range

of 400-4000 cm^{-1}. An optical properties and peaks of absorption were obtained by Perkin Elmer UV/VisSpectrophotometer Lambda 25 which operates in the ultraviolet and visible spectral ranges. The morphological analysis of samples was done by using Carl Zeiss SUPRA 55-VP FE-SEM with energy dispersive X-ray analysis (EDX) which was by Oxford Instruments X-MAX ($20mm^2$) for analyzing the composition elemental of the samples.

❖ SUMMARY OF RESULTS

- ### Structural Characterization of

The X-ray diffraction method was used to examine crystallite size and crystallinity for ZnO100% pure and ZnO-CuO NCPs thick film with different concentrations 10:0. 8:2, 7:3, 6:4, and 5:5 (in percentage ZnO100% pure; ZnO80%-CuO20%; ZnO70%-CuO30%; ZnO60%-CuO40%; and ZnO50%-CuO50%) for structural information. The diffraction patterns for each sample are displayed in **Figure 2.** Without any CuO concentration added, it was seen that just the peaks of ZnO were present, indicating hexagonal wurtzite structure i.e. a three-dimensional structure with lattice-like architecture that contains two atoms from various elements in alternating places. Strong bonds between the atoms are made possible by this arrangement, resulting in a hard and stable lattice. Because it has a high surface area to volume ratio and can store a lot of charge, this kind of structure is perfect for usage in semiconductor materials. The hexagonal wurtzite lattice can also endure high temperatures and pressures since the atoms are locked in place by strong bonds, which makes it valuable for a range of applications. The XRD identifies the Bragg's reflections at 2θ degree 31.72°, 36.16°, 47.45°, 56.56°, 62.79°, 66.340° 67.93°, 69.02°, and 76.96°corresponding to the Miller indices in the Cartesian coordinate system as (100), (002), (101), (102), (110), (103), (200), (201), (004), and (202) hkl planes respectively [68]. The X-ray reflections matches with JCPDS card No.01-079-0206 of ZnO bulk. The peaks of CuO started appearing at molar ratios (8:2, 7:3, 6:4, and 5:5) for ZnO:CuO NCPs thick film respectively which are indicated monoclinic structure of CuO at 2θ degree 31.70°, 38.76°, 48.50°, 56.56°, 61.52°, 62.88°, 66.11°, 68.03°, and 75.22° corresponding to the Miller indices (110), (100), (002), (111), (102), (-202), (110), (202), (103), (113), (200), (112), (201), and (-222) planes respectively [69], this is matched with JCPDS card No.00-041-0254 of bulk CuO.

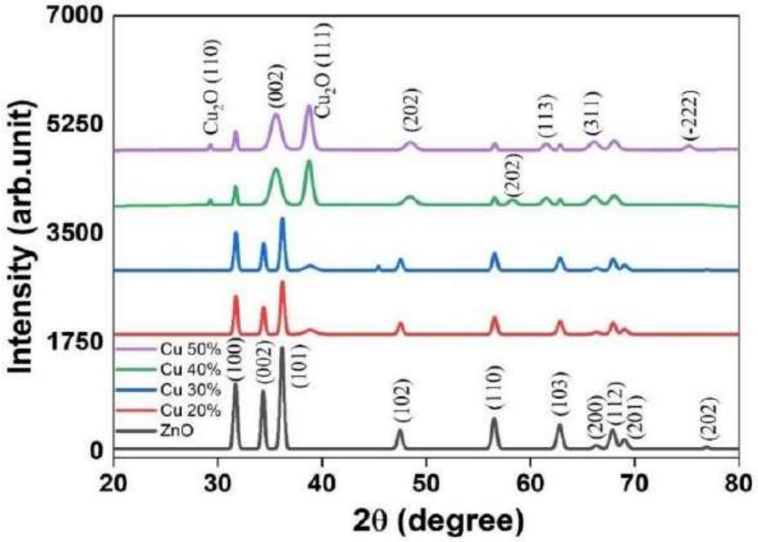

Figure 8. X-ray diffraction pattern of ZnO-CuO thick film

Table 2. Miller Indices (hkl), and Lattice Constant (a) of pure ZnO and ZnO-CuO thickfilm

ZnO					a = b				
h	k	l	2θ	θ	Sinθ	2Sinθ	d	(a/d)^2	a
1	0	0	31.724	15.862	0.273	0.547	2.818	8.846	2.818
1	0	1	36.162	18.081	0.310	0.621	2.481	11.406	3.509
1	0	2	47.453	23.726	0.402	0.805	1.914	19.171	4.280
1	1	0	56.563	28.281	0.474	0.948	1.625	26.581	2.299
1	0	3	62.792	31.396	0.521	1.042	1.478	32.135	4.675
2	0	0	66.340	33.170	0.547	1.094	1.408	35.445	2.815
1	1	2	67.931	33.966	0.559	1.118	1.378	36.960	3.376
2	0	1	69.021	34.511	0.567	1.133	1.359	38.007	3.039
2	0	2	76.963	38.482	0.622	1.245	1.238	45.849	3.500
									3.368

Table 3. FWHM and Crystallite Size D (nm) of pure ZnO and ZnO-CuO thick film

2θ	θ in Degree	Radian(θ)	FWHM Degree(θ)	FWHM Radian(θ)	Cos θ	D= 0.9λ/βCosθ	D nm
31.724	15.8621	0.277	0.40936	0.007	0.962	201.869	20.187
36.162	18.0812	0.315	0.4368	0.008	0.951	191.435	19.143
47.453	23.7264	0.414	0.50969	0.009	0.916	170.348	17.035
56.563	28.2814	0.493	0.52601	0.009	0.881	171.587	17.159
62.792	31.396	0.548	0.58397	0.010	0.854	159.448	15.945
66.34	33.17	0.579	0.56956	0.010	0.837	166.708	16.671
67.931	33.9655	0.593	0.64583	0.011	0.830	148.380	14.838
69.021	34.5106	0.602	0.63918	0.011	0.824	150.896	15.090
76.963	38.4816	0.671	0.07786	0.001	0.783	1303.901	130.390
34.372	17.1858	0.300	0.3624	0.006	0.955	229.594	22.959
							28.942

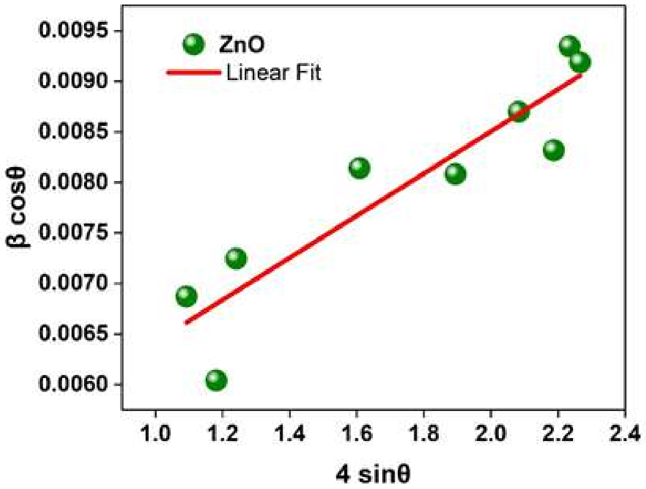

Figure 9. Williamson-Hall Plot of typical ZnO-CuO thick film

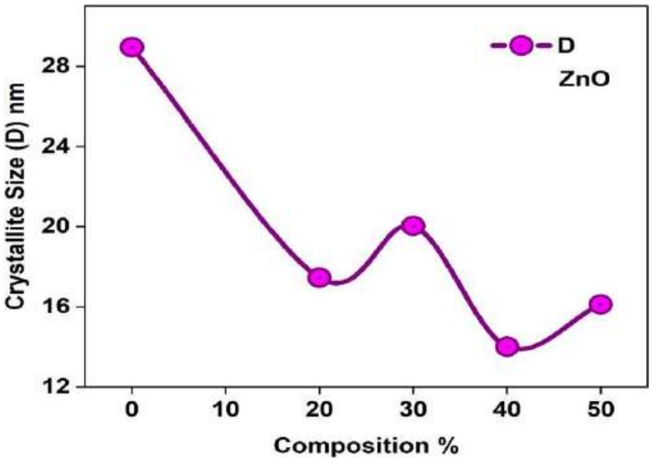

Figure 10. X-ray diffraction pattern of typical ZnO-CuO thick film

The increasing concentration of CuO led to an increase in the intensity of CuO peaks and a decrease inthe intensity of ZnO peaks [70] as shown in **Table 2.** According to D.M. Fernandes et al. the emergence of two phases for ZnO and CuO verifies the effective synthesis of NCPs [71]. The higher concentration of copper which has exceeded the 15 mol% led to the occurrence of peaks of the CuO phase. The calculation for the interplanar spacing (dhkl) was done by Bragg's Law [72] eq. (12)

$$n\lambda = 2d_{hkl} \sin\theta \qquad (12)$$

Where n =1 is the order of diffraction, λ= 0.15406 nm; is the wavelength of the X-ray, (dhkl) is the interplanar spacing and the θ is the angle between the incident ray to the crystal planes. The dislocationdensity δ is calculated by eq. (13) [73];

$$\delta = \frac{1}{D^2} \qquad (13)$$

Where (D) is the crystallite size. The results of interplanar spacing (dhkl) and dislocation density δ are shown in **Table 1**. Lattice Constants values a, b, and c are shown in **Table 2**, which matched with the reference database of Joint Committee on Powder Diffraction Standards (JCPDS) is a for crystallographic data for ZnO bulk materials, that contains information about the crystallographic properties of ZnO in bulk quantity. The peaks of CuO start appearing by adding its concentrations, still the dominant ZnO peaks exists with a hexagonal structure at ZnO80%-CuO20%; ZnO70%-CuO30%.

CONCLUSION:

This work used the chemical co-precipitation approach to manufacture ZnO-CuO NCPs thick film ZnO100% pure; ZnO80%-CuO20%; ZnO70%-CuO30%; ZnO60%-CuO40%; and ZnO50%-CuO50%.We achieved a successful nanocomposite. The samples have been submitted to several studies, including XRD, FE-SEM with EDX, UV-Vis absorption, and FTIR spectroscopy. XRD investigation revealed peaks for two structures associated to ZnO-CuO NCPs thick film, with smaller crystal size as CuO content increased. FE-SEM images indicated a heterogeneous structure composed of two metal oxides (ZnO and CuO), with agglomeration increasing with CuO concentration. UV-Vis absorption spectra show an improvement in absorption toward the UV region due to the emergence of a blue shift. FTIR spectra highlighted the key bonds that were present. The hysteresis plots of all the samples showed the ferromagnetic behavior. The saturation magnetization (Ms), coercivity (Hc), remanence magnetization (Mr), and magneton number (ηB) of the present samples were close to the best-reported values. The Raman analysis of the prepared sample ZnO-CuO NCPs thick film confirmed the hexagonal wurtzite and monoclinic structure formation with five active Raman modes i.e. A1g + Eg + 3T2g. The optical band gap determined from UV-Vis studies and Tauc plot is of the standard order. CuO/ZnO NCPs thick film led in the effective detection of several oxidizing and reducing gases.

REFERENCES:

[1] B. Purnama, A.T. Wijayanta, Journal of King Saud University-Science, 31 (2019) 956-960.

[2] S. Altabbaa, N.A. Mann, N. Chauhan, K. Utkarsh, N. Thakur, G.A.-E. Mahmoud, Nanotechnology for Environmental Engineering, 8 (2023) 481-498.

[3] I. Kang, J. Yang, W. Lee, E.-Y. Seo, D.H. Lee, Technology in Society, 74 (2023) 102326.

[4] S. Shah, P. Famta, D. Bagasariya, K. Charankumar, E. Amulya, D.K. Khatri, R.S. Raghuvanshi, S.B. Singh, S. Srivastava, International Journal of Pharmaceutics, (2022) 122101.

[5] P. Halappa, H.M. Rajashekar, C. Shivakumara, Journal of Alloys and Compounds, 785 (2019) 169-177.

[6] S. Pramanik, S. Mukherjee, S. Dey, S. Mukherjee, S. Das, T. Ghosh, P. Ghosh, R. Nath, P.K. Kuiri, Journal of Luminescence, 251 (2022) 119156.

[7] D. Han, X.-B. Li, D. Wang, N.-K. Chen, X.-W. Fan, Physical Review B, 105 (2022) 024104.

[8] A. Sathiyaseelan, K. Saravanakumar, X. Zhang, K.V. Naveen, M.-H. Wang, International Journal of Biological Macromolecules, 237 (2023) 124129.

[9] N. Elavarasan, S. Vignesh, M. Srinivasan, G. Venkatesh, G. Palanisamy, P. Ramasamy, B. Palanivel, A.M. Al-Enizi, M. Ubaidullah, V.R.M. Reddy, Journal of Alloys and Compounds, 906 (2022) 164255.

[10] M.A. Franco, P.P. Conti, R.S. Andre, D.S. Correa, Sensors and Actuators Reports, 4 (2022) 100100.

[11] R. Chauhan, A. Kumar, R. Tripathi, A. Kumar, Advancing of zinc oxide nanoparticles for cosmetic applications, Handbook of consumer Nanoproducts, Springer2022, pp. 1-16.

[12] Y. Wang, Z. Zheng, J. Wang, X. Liu, J. Ren, C. An, S. Zhang, J. Hou, Advanced Materials, 35 (2023) 2208305.

[13] A. Chatterjee, A. Ravindra, G.K. Kumar, C. Rajesh, Journal of the Indian Chemical Society, 99 (2022) 100653.

[14] H. Safdar, R. Aydın, B. Şahin, Ceramics International, 48 (2022) 26678-26688.

[15] P. Raju, Q. Li, Journal of The Electrochemical Society, 169 (2022) 057518.

[16] S.R. Mishra, M. Ahmaruzzaman, Sustainable Materials and Technologies, 33 (2022) e00463.

[17] R. Saadon, O.A. Azeez, Energy Procedia, 50 (2014) 445-453.
[18] K.-M. Kim, H.-R. Kim, K.-I. Choi, H.-J. Kim, J.-H. Lee, Sensors, 11 (2011) 9685-9699.
[19] S.R. Morrison, Sensors and Actuators, 2 (1981) 329-341.
[20] J.L. Santos, F. Farahi, Handbook of optical sensors, Crc Press2014.
[21] P. Tardy, J.-R. Coulon, C. Lucat, F. Menil, Sensors and Actuators B: Chemical, 98 (2004) 63-68.
[22] G. Korotcenkov, Conventional approaches, 1 (2013).
[23] B. Adhikari, S. Majumdar, Progress in polymer science, 29 (2004) 699-766.
[24] N. Wright, A. Horsfall, Journal of Physics D: Applied Physics, 40 (2007) 6345.
[25] J. Burgin, M. Liu, P. Guyot-Sionnest, The Journal of Physical Chemistry C, 112 (2008) 19279-19282.
[26] P.K. Sekhar, E.L. Brosha, R. Mukundan, F. Garzon, The Electrochemical Society Interface, 19 (2010) 35.
[27] A. Hulanicki, S. Glab, F. Ingman, Pure and applied chemistry, 63 (1991) 1247-1250.
[28] I. Simon, N. Bârsan, M. Bauer, U. Weimar, Sensors and Actuators B: Chemical, 73 (2001) 1-26.
[29] J.E. Thompson, Trends in Environmental Analytical Chemistry, 11 (2016) 23-34.
[30] O. Lupan, G. Chai, L. Chow, Microelectronics Journal, 38 (2007) 1211-1216.
[31] M. Stamataki, I. Fasaki, G. Tsonos, D. Tsamakis, M. Kompitsas, Thin Solid Films, 518 (2009) 1326-1331.
[32] H. Kim, J. Horwitz, S. Qadri, D. Chrisey, Thin solid films, 420 (2002) 107-111.